water

MDPI

Article

Tracing Nitrate-Nitrogen Sources and Modifications in a Stream Impacted by Various Land Uses, South Portugal

Mariela A. Yevenes [1,2,*], Karline Soetaert [3] and Chris M. Mannaerts [1]

[1] Faculty of Geo-Information and Observation Science, University of Twente, P.O. Box 217, 7500 AE Enschede, The Netherlands; c.m.m.mannaerts@utwente.nl

[2] Department of Oceanography and Center for Climate and Resilience Research, Universidad de Concepción, Casilla 160-C Concepción, Chile

[3] Department of Ecosystem Studies, Netherlands Institute of Sea Research, Postbus 140, 4400 AC Yerseke, The Netherlands; Karline.Soetaert@nioz.nl

* Correspondence: mayevenes@profc.udec.cl; Tel.: +56-41-2203-585

Academic Editors: David K. Kreamer and Y. Jun Xu

Received: 18 January 2016; Accepted: 29 August 2016; Published: 6 September 2016

Abstract: The identification of nitrate-nitrogen (NO_3–N) origin is important in the control of surface and ground water quality. These are the main sources of available drinking water. Stable isotopes (^{15}N and ^{18}O) for NO_3–N and along with a 1-D reactive transport model were used to study the origin and processes that lead to nitrogen transformation and loss in a major stream that flows into a reservoir within an intensively cultivated catchment area (352 km^2) in Alentejo-Portugal. Seasonal water samples (October–November 2008, March 2009 and September 2009) of stream surface water, wells and sediment pore water were collected. The results showed consistently increasing isotope values and decreasing NO_3–N concentrations downstream. During winter (wet period, November 2008 and March 2009) slightly higher NO_3–N concentrations were found in comparison to early fall (dry period: October 2008) and summer (dry period: September 2009). Isotopic composition of ^{15}N and ^{18}O values in surface water samples from the stream and wells indicated that the dominant NO_3–N sources were derived mainly from the soil and fertilizers. There was also significant nitrification in surface water at the head of the stream. Sediment pore waters showed high NO_3–N values near the sediment-water interface (reaching 25 $mg{\cdot}N{\cdot}L^{-1}$) and NO_3–N concentrations sharply decreasing with sediment depth, suggesting significant NO_3–N consumption. Denitrification was also detected using the ^{15}N signature in upstream waters, but not downstream where very low NO_3–N levels were measured. In the stream, the calculated isotopic enrichment factor for NO_3–N was $-2.9‰$ for ^{15}N and -1.78 for ^{18}O, this indicates that denitrification accounts for 7.8% to 48% of nitrate removal.

Keywords: nitrate-nitrogen; stable isotopes; streams; reactive transport model

1. Introduction

Recent studies suggest that the nitrogen (N) cycle is the most rapidly changing biogeochemical element and that the excessive use of reactive N in the environment is the third most important problem globally, after biodiversity loss and climate change [1,2]. One of the challenges concerning excess reactive N in the environment is a lack of understanding regarding the catchment scale of N removal, including the nutrient dynamics and their implications within different terrestrial and aquatic ecosystems [3–6]. An excess of reactive N in different environments can negatively impact water quality and cause an increase in the transfer of greenhouse gases to the atmosphere [7]. Streams impacted by agriculture may receive high levels of reactive N (i.e., nitrate, ammonium, organic nitrogen) from the land. Fundamentally, when moist agricultural soils are fertilized, rapid increases in N cycling may

occur, creating excessive N availability and enhancing the potential for nitrogen loss to streams [8]. NO_3–N is the predominant form of reactive nitrogen, highly soluble and readily leached from soils. Ammonium (NH_4–N) is also important, but less prevalent in the water as it is adsorbed predominantly by charged clay particles.

Several studies suggest that shallow streams and the associated pore water (water from underlying sediments) within intense agricultural areas may act as "hotspots"—i.e., areas that present disproportionately high reaction rates relative to the surrounding area [9]. Taking this into consideration, any biogeochemical process occurring in a stream may be highly efficient over relatively short distances. This emphasize that shallow streams are considered to be important biogeochemical transformations zones [10]. Denitrifying bacteria reduce nitrate (NO_3–N) via nitrite NO_2–N nitric oxide NO and nitrous oxide (N_2O) to the non-reactive dinitrogen gas (N_2), with organic carbon frequently acting as an electron donor [11]. Denitrification is considered to be a particularly challenging process to measure and model [4]. Predominantly due to the fact that small sites (hotspots) frequently account for a high percentage of the denitrification activity, which depend on environmental factors such as substrate availability, temperature, and oxygen concentration in aquatic ecosystems. Although some of the removal and storage of reactive N occurs within the landscape, a significant proportion is thought to occur within surface water from streams and groundwater [12].

Dual stable isotope signatures of dissolved NO_3–N together with reactive transport modelling are both powerful tools to study the sources and processing of nitrate in streams, due to the fact that various origins and processes tend to have distinct isotopic signatures [13–15]. For instance, during denitrification as NO_3–N levels decrease, as a result of natural isotopic fractionation residual NO_3–N becomes enriched in heavy isotopes ^{15}N and ^{18}O [16,17]. This is because bacteria preferentially reduce $^{14}NO_3$ rather than $^{15}NO_3$, therefore leaving an enriched pool of $^{15}NO_3$ [18,19]. Despite the recently identified challenges and drawbacks regarding the isotopic identification technique, such as assumptions on oxygen sources in microbial nitrate [20], it continues to prove itself as a successful technique in identifying mixing sources [8,16].

The NO_3–N concentrations in European watersheds have been well documented [21–23], mainly due to concerns generated from the European Water Framework Directive [17,19,24]. However, in Southern Portugal, there is a lack of understanding about how the spatial and temporal patterns along a stream and in the underlying sediments relate to the intense land uses in the catchment area. To address this knowledge gap, stream water, well samples and underlying sediments were analysed for chemical and physical parameters, and NO_3–N isotopic ratios in the Roxo catchment, Southern Portugal. This information was used to identify the processes that lead to nitrogen transformation and loss along the length of a shallow stream, and to identify the sources of NO_3–N in the watershed, in surface waters of shallow streams, and in the sediment pore waters.

2. Methodology

2.1. Study Area

A mesoscale catchment area, the Roxo, in Southern Portugal (37°46′44″ N to 38°02′39″ N latitude and 7°5′47″ E to 8°12′24″ E longitude, Figure 1) was selected due to the intensive agricultural cultivation practices in the area. The Roxo catchment area is 352 km^2 and located in the Beja Province of the Alentejo region. A network of shallow streams that cross most of the agricultural area characterizes it. The Chaminé stream as a main stream was selected. It has a generally low flow volume (average 0.3 $m^3 \cdot s^{-1} \pm 0.02$) and with seasonally intermittent high flows occurring during autumn or winter. Annual rainfall during the study period from 2008 to 2009 was 547 mm, with the majority of the rainfall occurring between November and March. Mean annual temperatures were around 22 °C. Soil categories, according to the FAO-UNESCO system, are characterized as Luvisols, Litosols, Planosols and Vertisols, with Luvisols being the main soil class present in the area [25,26]. Hydro-geological studies in the northern part of the catchment boundaries indicated that a productive aquifer of the

upper Roxo catchment is located in the Beja-Acebuches and Beja Gabbro geotectonic complexes. These geological formations represent mainly gabbro-dioritic rocks. This characteristic bedrock varies locally and can reach 30 m in thickness. This creates an unconfined aquifer with a shallow water table of 2 m approximately in the north with NO_3–N concentrations reaching 6.5 mg·N/L [27]. Near to the reservoir the water table is close to 6 m. The topography varies from nearly flat to a gently sloping terrain with elevations ranging from 123 m at the catchment reservoir outlet, to 280 m.a.s.l. near Beja city, over approximately 15 km distance. Water in the catchment area drains into the Roxo reservoir (max. volume approx. 10^8 m^3), an artificial impoundment built in the early 1960s and used for municipal water supply to Beja city (approx. 161,000 inhabitants), and also to the local mining industry and irrigation water supply to several irrigation perimeters [28]. The residual municipal waters from Beja city are channelled into a wastewater treatment plant (WWTP), before the residual effluent waters are released into the Chaminé-Pisoes streams in the upper part of the catchment. This yields an additional and relatively constant nitrogen input and loading on the upper catchment streams. Water quality in the catchment is affected by agriculture (80% of the catchment), with major crops such as winter wheat, maize, sunflower, cork and olives (Table 1, extracted from [29]).

Table 1. Land use, cover, and crop management information in the upper Roxo catchment area [29].

Land Use	Crop Information	Total Area (%)	Fertilizer Use	Fertilizer Type or NPK	Amount	Timing Dates
Agricultural-arable land winter annual in rotation	Maize	7.7	Planting Boost Mid/maturing	15-35-00 6-20-18 Nitro 32N	100 300 400	June–August
		5.4	Planting Development	20-20-00 Nitro 27	200 200	June–August
		19.5	Planting Development3 leaves stage	10-30-00 Nitro 27	300 250	Begin November January–February
Agricultural mixed crops	Summer annuals pasture, long fallow	36.8	–	–	–	–
Agricultural permanent crops	Olives Vineyards Cork oak	7.2 1.8 6.6	–	–	–	–
Water bodies	Ponds, reservoir (dam)	3.0	–	–	–	–
Seminatural vegetation forest land	Rangeland Shrubs eucalyptus, Pinus	4.1 8.0	–	–	–	–
Urban	Urban low density Urban high density	0.10 0.15	–	–	–	–

Fertilization in the catchment is mainly maize from June to August, September, reaching 400 kg·ha^{-1} winter wheat reaching 300 kg·ha^{-1} at the beginning of the plantation every October, and alfalfa planted in June reaching 200 kg·ha^{-1}. Winter wheat is an intensive agricultural crop, generally requiring around 200 kg·N·ha^{-1} of Nitro 27% fertilizer, whereas the recommended Nitrogen fertilization for maize is 300 kg N·ha^{-1} of NPK [27,30]. The major fertilizer application in the catchment area occurs in June.

In the South of the catchment area 28% of the land is made up of Eucalyptus and Pine forest plantations, and some other areas have natural vegetation (Figure 1). High NO_3–N levels are observed in the drainage system, especially in the shallow aquifer of the Roxo catchment [31]. Further activities, such as pig, cattle and sheep farming also take place within the catchment area.

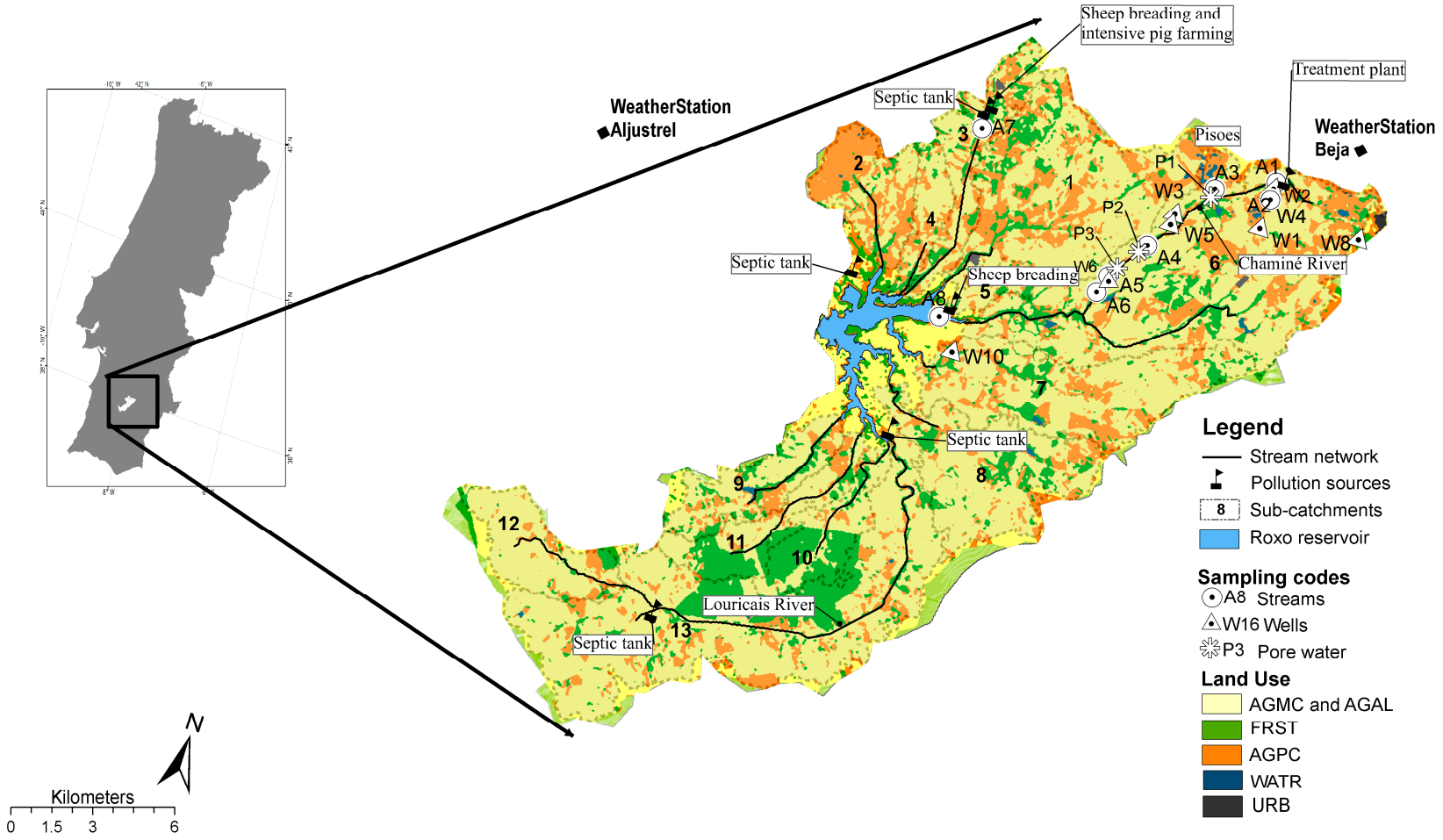

Figure 1. Location of the Roxo catchment study area, Southern Portugal, with the principal pollution sources. Circles are the sampling sites, including stream water (A), shallow groundwater (W), and pore water samples (P). A1–A9 are the stream sampling sites.

2.2. Water Sampling

Figure 1 shows a map of the major and perennial stream, indicating sampling point positions. Samples were collected midstream from 8 stream sites (A1 to A8 from upstream to downstream in the main Chaminé stream, along 15 km), and from 10 shallow wells with water table levels between 2 and 5 m. The discrete water sampling campaigns were conducted during dry and wet periods referred to summer (from 19th to 29th October 2008 and from 3th to 15th September 2009) and winter (from 1st to 7th November 2008, 15th to 26th March 2009), respectively. Three replicate 15 mL water samples were collected from each monitoring sampling point for nutrients (NO_3–N, NH_4–N) and 100 mL water samples for stable isotopes (^{15}N and ^{18}O), using a peristaltic water pump, connected to a water collector and filtered in the field with 0.45 µm filters. Water samples for nutrients and stable isotopes were collected in non-reactive plastic bottles with double seal caps and stored on dry ice to keep frozen for transport back to the laboratory. Analysis took place immediately after every sampling trip. O_2, Temperature (°C) and Electrical conductivity (EC) were measured in the field with a hand-held Hanna multi-parameter instrument.

Sediment pore water was sampled at three sites of the Chaminé stream (Figure 1). Sediment porewater profiles were sampled with minimum disturbance by inserting a rhizon sampler syringe [32] into drill holes in a 52 cm long core located at the bottom of the stream pools (P1, P2 and P3), near to sites A3, A4 and A6. The holes were slightly bigger than 4 mm diameter size to allow fixing the Rhizon samplers through the drill holes. The holes were sealed with duct tape prior and during the sediment collection. After the collection, a needle was used to pierce the tape and introduce each Rhizon sampler. Subsequently, ten Rhizon samplers were inserted horizontally into the core at depths of 0, 0.5, 1, 2, 3, 5, 7, 10, 25 and 30 cm below the sediment-water interface. Samples were stored directly in 10 mL glass vials without contact with the atmosphere.

Cations and anions concentrations were analysed by inductively coupled plasma-optical emission spectrometry (Varian Liberty AX sequential ICP-AES and a Varian SpectrAA Atomic Absorption Spectrometer (AAS) (Varian Inc., Palo Alto, CA, USA), at Faculty of Geo-information Science and Earth Observation, ITC/University of Twente, Enschede, The Netherlands. Water samples collected for isotopic composition (^{15}N and ^{18}O) were analysed using the bacterial denitrification method [33] and determined by isotope ratio mass spectrometry on a Sercon 20-20 IRMS with Syscon Electronics (Sercon Ltda, Cheshire, UK) in the certified ISOFYS Environmental Isotope laboratory of Ghent University (Belgium).

2.3. Stable Isotope Calculations

The isotopic results are expressed using the delta notation (i.e., the difference in parts per thousand between the less abundant isotopic ratio and the most abundant isotopic ratio, relative to the same ratio in a reference standard (Vienna Standard Mean Ocean Water for ^{18}O and an open atmosphere air standard for ^{15}N), and defined by:

$$^{15}N = 1000[(R_{sample} - R_{air})/R_{air}]; \; ^{18}O = 1000[(R_{sample} - R_{smow})/R_{air}] \quad (1)$$

where R_{sample} and R_{air} and R_{smow} are the isotopic ratios ($^{15}N/^{14}N$ or $^{18}O/^{16}O$) for the sample and for the reference standard of ^{15}N and ^{18}O, respectively.

Partitioning of isotopes between two compounds containing the same element with different isotopic ratio is called isotope fractionation [18] and can be defined through the kinetic fractionation factor as follow:

$$\alpha\,(p - s) = R_p/R_r \quad (2)$$

where α represent the kinetic fractionation factor between the product (p) and the substract (s), R_p and R_r are heavy to light isotope ratios ($^{15}N/^{14}N$) in the product (residual nitrate) and reactant (or substrate), respectively [16]. Biologically mediated denitrification enriches the residual in both

^{15}N and ^{18}O; whereas other sinks result in little or no enrichment. Therefore, the magnitude of ^{15}N enrichment associated with nitrate removal is quantified through an enrichment factor. The kinetic fractionation factor is typically described in terms of an enrichment factor (ε) as follows:

$$\varepsilon = (\alpha - 1) \times 1000 = ((\delta p - \delta_r)\delta_r + 1000) \times 1000 \quad (3)$$

where δ_p and δ_r are delta values of the product and reactant, respectively. The enrichment factor is negative for most of the nitrogen transformation processes, and in the case of denitrification it has been defined with a range from $-40‰$ to $-3.5‰$, which reveals a variety of environmental and experimental conditions [34–36].

The enrichment factor can be estimated from the evolution of the isotopic composition of the residual reactant [18] defined as:

$$\partial_r = \partial_{r0} + \varepsilon \ln(NO_3 - N) \quad (4)$$

where ∂_r is the ^{15}N or ^{18}O value of the reactant nitrate at time t, ∂_{r0} is the initial ^{15}N or ^{18}O value of the nitrate, (NO_3) is the remaining fraction of nitrate, and is the fractionation or enrichment factor [16]. Enrichment factors for ^{15}N and ^{18}O in surface waters were determined by regression of ^{15}N or ^{18}O on ln(NO_3–N). Finally, the ∂_r values are transformed to percentages (%) to obtain the degree of denitrification for each sampling point [37]. To calculate the degree of denitrification from our data, the initial isotopic composition (∂_{r0}) was chosen to be the lowest ^{15}N value during the samplings.

2.4. Reactive Transport Model

A simple reactive transport model was developed to reproduce the sampling data from 2008 to 2009. We assess the dynamics of dissolved inorganic nitrogen (i.e., NO_3–N and NH_4–N) in the surface water, through a 1-D reactive transport model for the main stream (Chaminé) of the Roxo catchment area (approx. length 15 km). The one dimensional reactive transport model was developed in the open source software R [38]. The R package ReacTran [39] allows the use of the volumetric advective-diffusive transport function and the reaction-advection equation for a substance given as [40]:

$$(\partial C_i)/t = -(1\partial QCi)/(A_x \partial_x) + REAC_i \quad (5)$$

where t is time, and x is the distance along the stream axis, the first term represents transport by the stream flow (advection) and the second term represents (turbulent) dispersion. An assumption is made that the cross-sectional area (A_x) is constant in time [41], but it varies along the stream axis (x). The chemical state variables in the reactive advection dispersion model C were described in terms of concentration (mg·N·L^{-1}). REAC$_i$ are the main reactions, comprising nitrification and denitrification modeled where:

$$REAC_{NO3} = \text{Nitrification} - \text{Denitrification, and } REAC_{NH3} = -\text{Nitrification} \quad (6)$$

boundary conditions for nitrate and ammonium were derived from stream campaigns; upstream and downstream [42]. Nitrification and denitrification rates were taken from the literature. The upstream boundary conditions were specified as follows: the upstream ammonium concentration was taken as 1.1 times the maximal measured nitrate concentration along the stream, while the upstream nitrate concentration was set to be 0. Stream flow was measured in the sampling sites when the water level was sufficient for measurements to be taken. Furthermore, data on the daily streamflow were obtained using precipitation, evapotranspiration, and reservoir storage volume and water use databases, using an inverted reservoir water balance approach. This procedure is based on the estimation of the reservoir inflow, taken from the variation over time of the storage volume of the reservoir and the total outflow from the reservoir [43]. The required rainfall data from 2008 to 2009 was obtained from automatic weather stations located close to the Beja and Aljustrel (Figure 2). Water depth was generally very low (0.1 to 0.5 m) in the streams, and was measured during the fieldwork campaigns. The model was

implemented in the open source software R using R-package ReacTran [39]. It was solved assuming that the concentrations had reached steady-state [39].

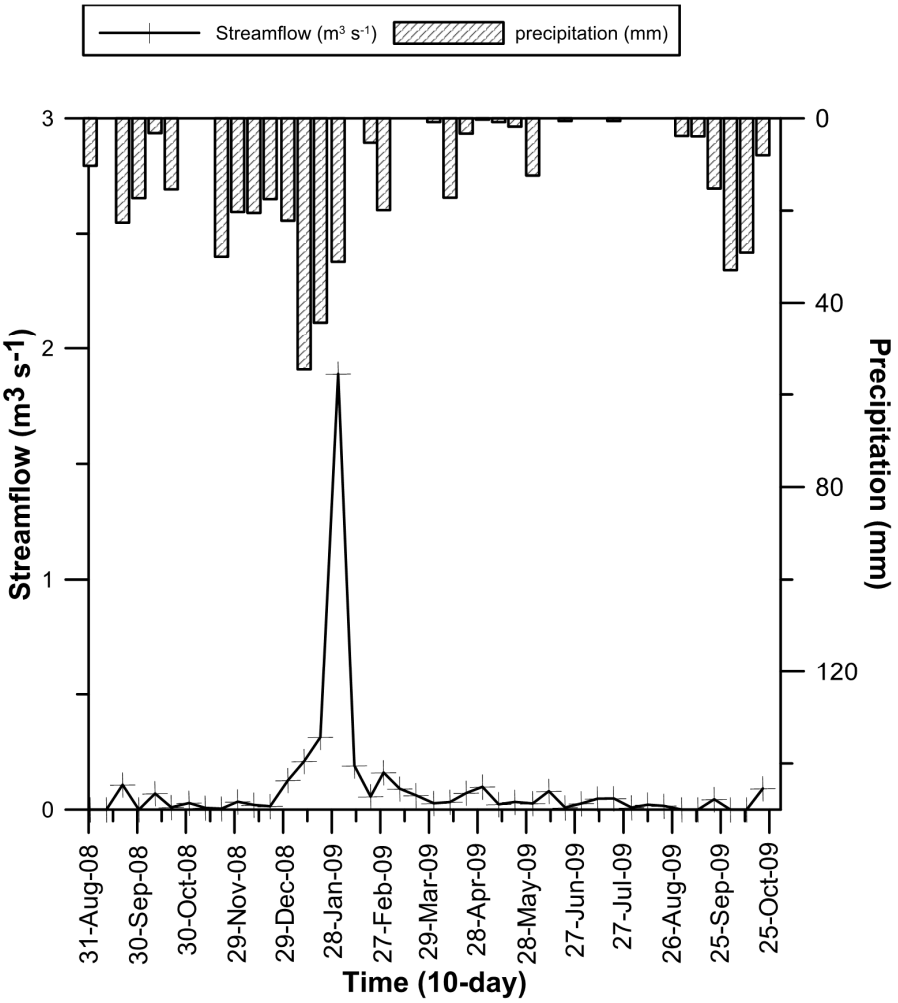

Figure 2. Rainfall (mm) and streamflow ($m^3 \cdot s^{-1}$) data in the Chaminé stream in the Roxo catchment.

3. Results

3.1. Solutes and Reactive Transport Modelling

Table 2 summarizes the values from physical and chemical parameters taken over three field campaigns to the streams, pore water and wells (shallow groundwater). The streamflow regime is characterized by slow flow velocities (average 0.1 to 0.2 m/s) and shallow flow depths ranging from 0.05 to 0.5 m, depending on the shape of the local stream cross section. Average annual flow (2003–2009) was 0.10 $m^3 \cdot s^{-1}$, with seasonal low values at the end of summer of 0.04 $m^3 \cdot s^{-1}$. High daily flow peaks are typically recorded at the end of winter and reached values of up to 1.89 $m^3 \cdot s^{-1}$ in the February 2009 field campaigns. Stream water temperature averaged 23 $\pm$ 8 °C during the entire period and electrical conductivity (EC) varied seasonally with values ranging from 789 $\mu S \cdot cm^{-1}$ in March 2009 to 3110 $\mu S \cdot cm^{-1}$ in September 2009. Stream water showed slightly basic pH values, with an average value of 8.24 $\pm$ 0.88. Dissolved oxygen levels in October and November 2008 were on average 6.0 $\pm$ 1.7 $mg \cdot O_2 \cdot L^{-1}$ and 7.7 $\pm$ 1.4 $mg \cdot O_2 \cdot L^{-1}$, with oxygen significantly increasing in a downstream direction towards the reservoir.

Table 2. Measured values (mg·L^{-1}) for nutrients (nitrate-nitrogen, ammonium-nitrogen) and dissolved oxygen, (‰) for stable isotopes, (µS·cm^{-1}) for electrical conductivity and (°C) for temperature. Descriptive statistics of chemical variables in the stream water, shallow groundwater, and pore water samples during the study period (October–November 2008, March 2009 and September 2009).

Element	October 2008				November 2008				March 2009				September 2009			
	Max	**Min**	**Average**	**SD**	**Max**	**Min**	**Average**	**SD**	**Max**	**Min**	**Average**	**SD**	**Max**	**Min**	**Average**	**SD**
Streams																
NO_3	16.5	1.27	7.34	5.23	16.7	1.68	8.32	5.18	15.2	0.44	5.7	5.48	10	0.30	3.32	3.53
NH_4	10.7	<	1.2	3.6	10.9	<	2.3	2.9	45	0.05	3.9	11	0.45	<	0.2	0.15
^{15}N	11.3	3	7.5	2.9	-	-	-	-	15.1	3.2	7.0	3.9	13.7	4.4	7.8	4
^{18}O	31.1	4.9	15	7.8	-	-	-	-	9.8	4.3	6.4	1.9	13.1	9.1	11.2	1.8
DO	9.3	2.2	6.0	1.7	9.8	3.7	7.7	1.4	15.2	0.04	5.7	5.5	9.8	2.1	6.7	1.9
T	25.8	15.8	20.8	3.4	19.8	14.7	18.3	2.9	20	13	15.8	2.0	30.4	19.1	25.9	3.9
EC	2100	789	1432	483	1890	760	1340	384	1854	685	1190	291	3110	543	1390	676
Wells																
NO_3	20.2	1.7	10.3	8.2	-	-	-	-	25.5	2.2	9.8	8.6	18.2	0.03	6.8	8.4
NH_4	4.5	0	0.8	1.8	-	-	-	-	0.5	0.04	0.2	0.2	0.45	0	0.18	0.2
^{15}N	-	-	-	-	-	-	-	-	20.5	3.29	8.9	5.7	10.5	3.3	6.9	2.6
^{18}O	-	-	-	-	-	-	-	-	15.1	4.33	7.5	3.5	7.4	4.3	6.2	1.2
DO	9.3	3.4	5.9	2.2	-	-	-	-	25.5	2.21	9.8	8.6	8.3	4.5	6.2	1.5
T	23.5	19.7	21.4	1.6	-	-	-	-	18.5	14	16	1.5	24.4	20.8	21.9	1.7
EC	1626	507	873	389	-	-	-	-	996	664	848	108	996	664	832	110

Note: < means below limit of detection in the sample.

Concentrations of NH_4–N decreased significantly in the upper reaches of the stream, while nitrate increased (Figure 3a). NO_3–N concentrations ranged from 0.3 to 16.5 mg·N·L^{-1}, with mean values of 7.34 ± 5.23 in October 2008, 8.32 ± 5.18 during November 2008, 5.70 ± 5.48 during March 2009, and 3.32 ± 3.53 mg·N·L^{-1} during September 2009 (Table 2). The highest NO_3–N concentrations were registered in the second (A2) and third (A3) stations after which they decreased through the Chaminé stream towards the downstream (Figure 3b), where nitrate values were close the detection limit (<0.1 mg·N·L^{-1}). NO_3–N concentrations in shallow groundwater (wells) were generally higher than in streams, ranging from 0.1 to 25.5 mg·N·L^{-1}. The advection-reaction model was effective at capturing these trends (Figure 3). The model estimates the nitrate dynamic along the stream (distance 15 km) from upstream (A4) to downstream (A25), and provides satisfactory estimates for the first-order nitrification and denitrification rates, as 15 kg·day^{-1} and 1 kg·day^{-1} respectively (Figure 3c,d).

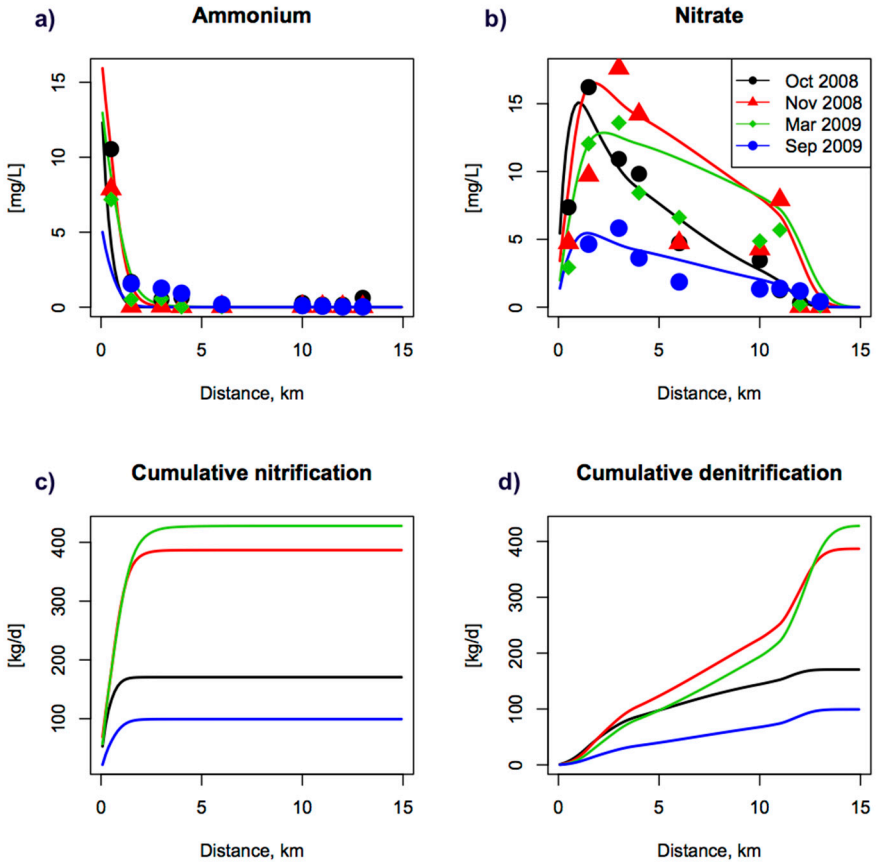

Figure 3. Simulated (line) and measured (circle) concentrations of nitrate-nitrogen and ammonium-nitrogen in the main stream (Chaminé river). From October 2008 to September 2009. Distance refers to the length of the river, from upstream (0 km) to downstream (15 km) versus (**a**) Ammonium concentration; (**b**) Nitrate concentration; (**c**) Cumulative nitrification; and (**d**) Cumulative denitrification. Black line and circles refer to October 2008, red line and triangles refer to November 2008, Green line and diamonds are associated to March 2009 and blue line and circles refer to September 2009.

NO_3–N fluxes in the stream ranged from 0.3 to 510 kg·NO_3–N·day^{-1} during the entire period. In October and November 2008, the fluxes ranged from 20.5 and 70.3 kg·NO_3–N·day^{-1} downstream to 448 and 304 kg·NO_3–N·day^{-1} upstream, but the highest values were recorded in March (510 kg·NO_3–N·day^{-1}) and the lowest in September 2009 (0.3 kg·NO_3–N·day^{-1}). The intermittent tributary has a likely influence during winter when mostly rainfall events acted. The estimated mass flux for the tributaries between October and November 2008 was between 9.62 and 43.38 kg·NO_3^-·day^{-1}. In March 2009 were found the highest values with 85.2 kg·NO_3^-·day^{-1}.

3.2. Sources of Nitrate-Nitrogen in Stream Surface Waters

Isotopic composition of N (^{15}N) ranged from 3.02‰ to 15.1‰, averaging 7.40‰. The oxygen isotope ^{18}O ranged from 4.29‰ to 30.9‰ and averaged 11.3‰. Nitrate isotopic values were always below detection limit downstream (Table 1, Figure 4), due to the systematically low nitrate concentrations observed in these locations. Values of ^{15}N and ^{18}O from stream water, with theoretical distributions of rain water, fertilizer, soil NH_4^+, and septic and manure sources, presented linearly plotted ^{15}N and ^{18}O values in stream water, in a ratio close to 1 (0.44). The positive relationship (0.44) between ^{18}O and ^{15}N indicated the occurrence of denitrification.

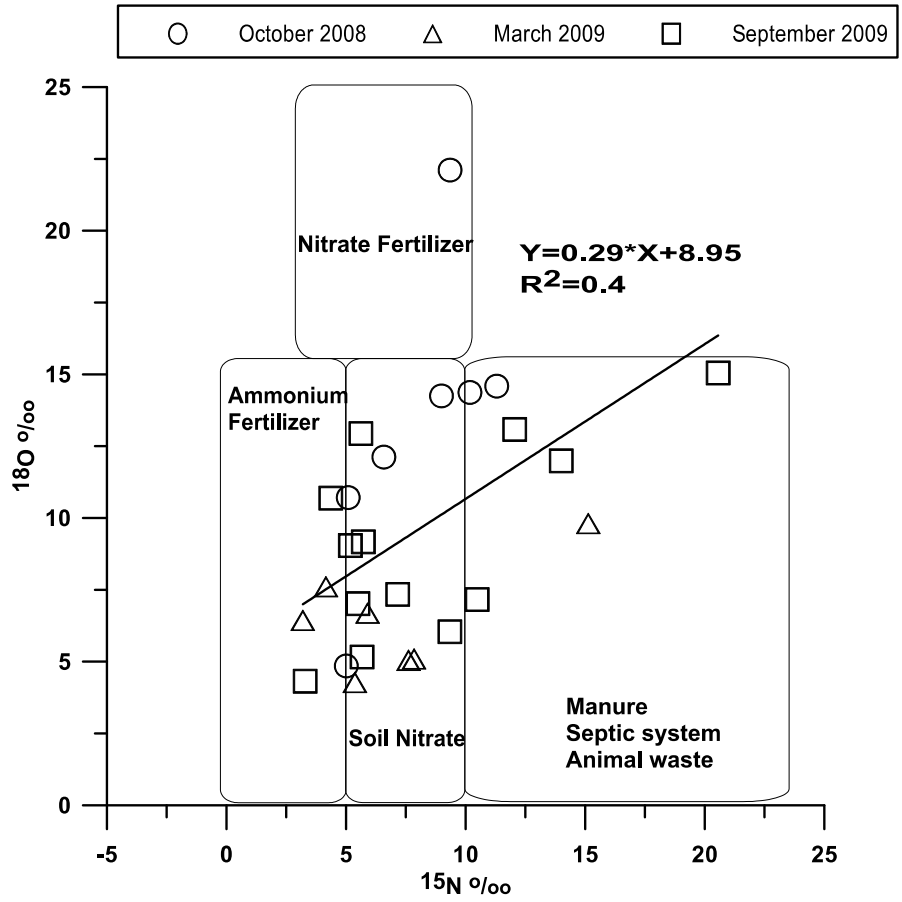

Figure 4. Ranges of nitrogen and oxygen isotopic composition for nitrate-nitrogen sources. The domain of soil nitrate is shaded (dark) and manure sources and ammonium fertilizers (lightest). The long line represents a denitrification vector, as denitrification progresses, the nitrogen and oxygen isotopic values of the remaining nitrate progressively increase in the direction of the vector (Kendall and McDonnell, 1998).

The relationship between ln(NO_3–N) and ^{15}N values followed the Rayleigh curve, with a negative enrichment factor ($\varepsilon = -2.9$‰ for ^{15}N and $\varepsilon = -1.5$‰ for ^{18}O) expressed by the regression analysis shown in Figure 5. According to the Rayleigh equation, denitrification contributions ranged from 7.8‰ to 49‰, both maximum and minimum values were recorded during the wet period (March 2009), with a total average of 16‰ ± 5‰ (Table 2). In the case of shallow groundwater from wells, dual isotope analysis for wells showed that ^{15}N and ^{18}O values ranged from +0.64‰ to +20.56‰, and −0.20‰ to 15.06‰, respectively (Table 2). Many of these values are close to zero, reflecting nitrate from reduced N fertilizers and from soil organic nitrogen. Figure 6 showed that most of the NO_3–N/Cl^- ratios with Cl^- concentrations do not correspond to the ranges for sewage and manure.

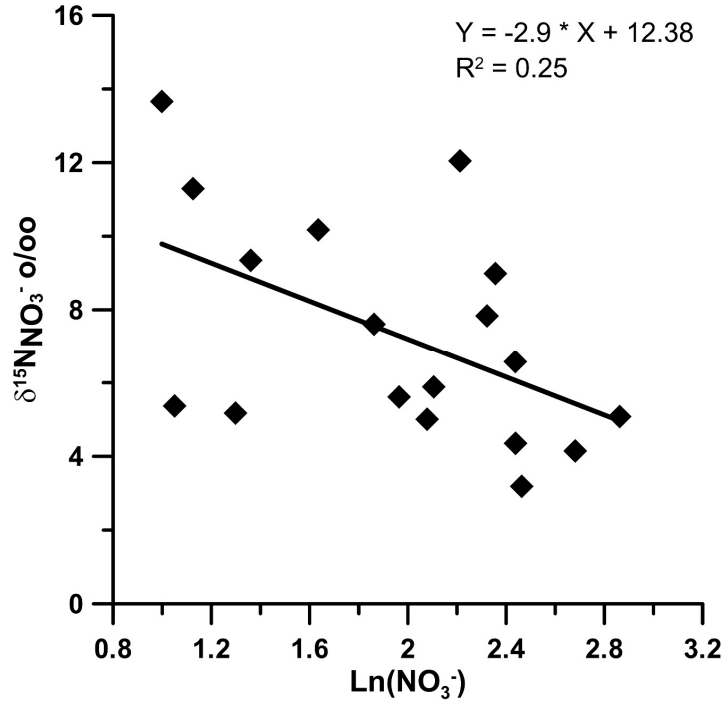

Figure 5. Linear regression of ^{15}N on ln(NO_3), where ln(NO_3) is the fraction of the original pool of nitrate still present. The slope of the regression is equal to the isotopic enrichment factor ε (here −2.9‰) for denitrification in the streams.

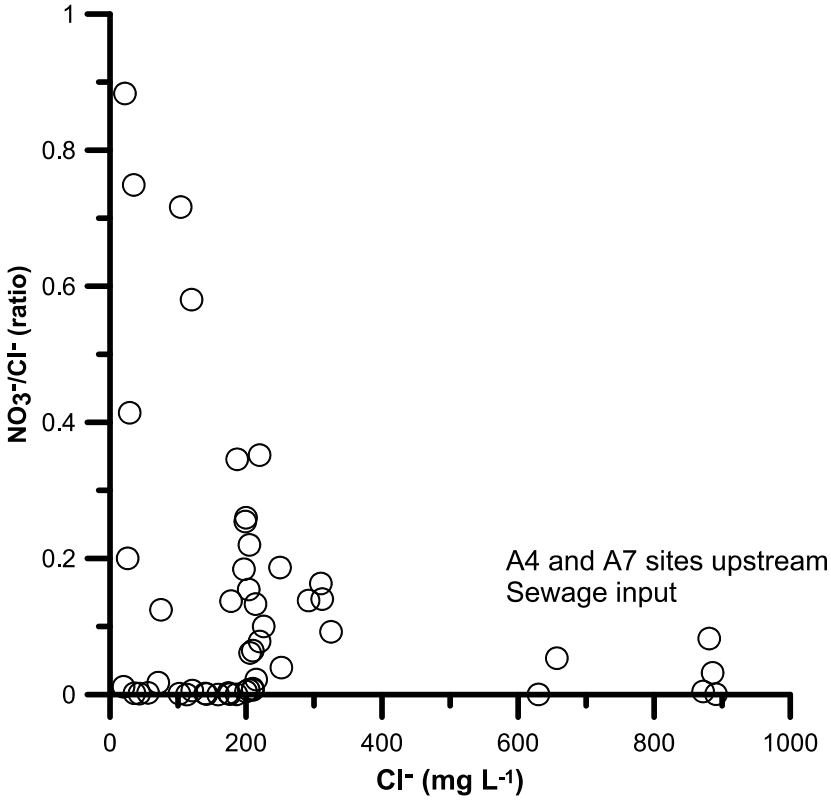

Figure 6. Chloride nitrate-nitrogen ratio in stream waters from the Chaminé stream.

3.3. NO_3-N Distribution in the Pore Waters

Pore water nitrate measurements from core sediments were obtained from three pools with rhizon samplers (Figure 7). The first pool (P1), located near the A3 sampling point, presented high nitrate values near the sediment-water interface (reaching 15 mg·N·L^{-1}), and a sharp decrease in nitrate with depth, where high levels of organic matter (around 20%) are characteristic of the area It suggested significant nitrate consumption in the sediment. In the second and third pool (P2 and P3), lower nitrate values (0.90 ± 0.37 mg·N·L^{-1}) were found in the first centimeters with little or no decrease with sediment depth, indicating that denitrification in the sediment was probably limited by nitrate. During winter sampling mean *T* °C, EC, and pH in the shallow wells corresponded to 15.8 ± 1.5 °C, 850 ± 113 µS·cm^{-1} and 7.9 ± 0.39. This was lower than in summer, with averages of 22.7 ± 1.99 °C, 1290 ± 896 µS·cm^{-1} and 9.23 ± 0.73, which reflects a longer residence time in summer than in winter. Dissolved oxygen content fluctuated widely, ranging between 2.18 and 10.4 mg·L^{-1} in winter and between 4.5 and 8.3 mg·L^{-1} in summer (Table 2).

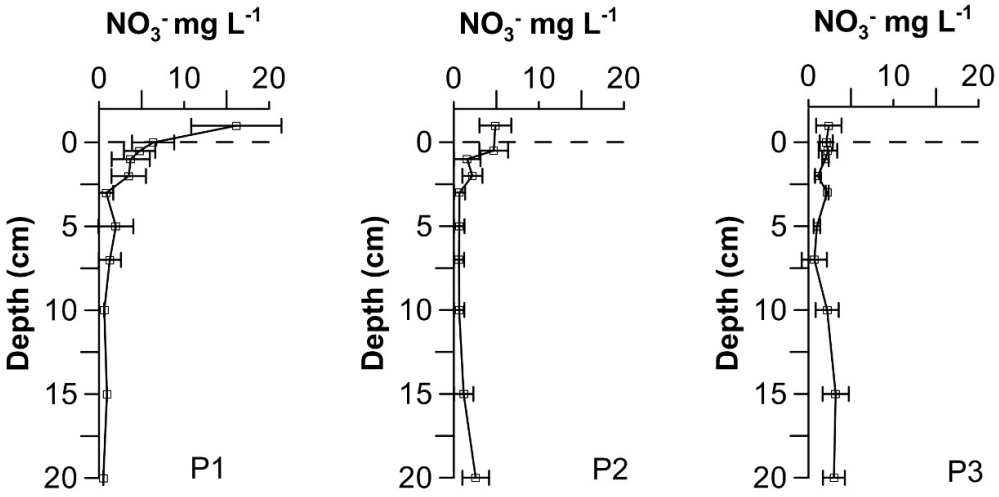

Figure 7. Average nitrate-nitrogen pore water measurements in three pools along the main stream of the Chaminé River. P1, P2 and P3 are pore water-sediment cores from each sampling point.

4. Discussion

We studied the nitrogen sources and transformations in the upper 15 kilometres of Chaminé stream, flowing through an area of intensive agricultural activity, based on concentration, stable isotopic composition data and reactive transport modelling. The modelling was included to assess the consistency of the observed data and to evaluate the impact of along-stream transport compared to biogeochemical transformations, while the stable isotopes were used to identify origin and main processes in the stream water.

The mean cross-sectional area fluctuates from around 1–3 m^2 in the first 11 kilometres, after which the stream rapidly broadens to 16 m^2 wide at 15 km distance, the total volume of this stretch is 257,000 m^3, of which less than 20% is in the first 10 km. The mean discharge is 0.3 m^3/s and flow velocities vary between 0.19 and 30 cm/s. It takes approximately 17 h for water to travel the first 10 km, and almost 10 days to reach the 15 km point.

4.1. Inorganic N in Surface Waters

Records show the occurrence of very high ammonium values at the first sampling point, due to a considerable ammonium input from waste waters originating from the treatment plant outfall, which is located ~500 m upstream from the sampling point. Subsequently, ammonium levels sharply decrease downstream, while nitrate concentrations increased. The high ammonium concentrations observed at

the first sampling point and rapid decrease in concentration throughout in the first few kilometres was clearly recorded with a simple advection-reaction model, the ammonium concentration was set at the upstream boundary as equal to 1.1 times the maximal observed nitrate concentration (5–15 mg·L^{-1}). This consistency between the nitrate peak and ammonium drop showed that ammonium was rapidly consumed and converted into nitrate due to nitrification occurring in the stream. The data from all sampling excursions were consistent with the model, assuming a high first-order consumption rate of ammonium of 25 kg·day^{-1}, which is in agreement with the range of nitrification rates often used in sediment biogeochemical models [44]. For every mole of ammonium converted to nitrate, two moles of oxygen are consumed, so the drop of 5 to 15 mg·L^{-1} ammonium in the first few kilometres of the stream is accompanied by an oxygen consumption of about 25–75 mg·L^{-1}. Based on the modelled nitrification rates, an oxygen consumption rate of 350–2000 mg O_2/L/day is estimated for the first kilometre, with oxygen concentrations in the order of 3 mg·L^{-1}, which is an exceptionally high rate. Remarkably, the high oxygen consumption rates due to nitrification were not reflected in the oxygen concentrations, which sharply increased between the first two sampling points. This indicates that re-aeration was much stronger than the oxygen consumption during nitrification (Figure 3). A simple extension of the advection-reaction model, where the reaeration flux was modelled as a function of the deviation of the oxygen concentration from saturation, showed that very high aeration rates (~100 day^{-1}) are necessary to trigger an increase in oxygen concentrations in this part of the stream (results not shown). Downstream from the site of nitrification, the ammonium concentrations remained very low. Overall it was estimated that 90 to 390 kg of NH_4–N enters the stream per day, all of which is converted to nitrate in the upper 2 kilometers.

Excluding the upstream sampling point, NO_3–N was the major ion compared to NH_4–N in the shallow stream. Concentrations sharply increased from low values to values well over 15 mg·L^{-1}, after which the concentration decreased in a downstream direction until it almost zero downstream. The fact that this decline was accompanied by a consistent increase in the ^{15}N isotope abundance in the pool NO_3–N identifies that nitrate loss is due to denitrification to nitrogen gas, rather than from dilution [7,35,37,45]. In the model, the decline of nitrate was reproduced with a first-order nitrate consumption rate of 1 kg day^{-1}, again comparable to parameters often used in sediment models (e.g., 0.2–3.5 kg·day^{-1}) [46]. This smears the zone of denitrification over a stretch from 2 km up to about 13 km downstream, after which the nitrate was almost entirely diminished. Note that total denitrification increases significantly and nitrate concentrations drop more prominently around 11 km from upstream. At this point the stream widens and residence time increases, hence a more pronounced imprint of denitrification on nitrate. Similar to the nitrification rates, it was estimated that 90 to 390 kg of NO_3–N are removed per day in the stream.

On the other hand, the studied area is mostly flat to undulating, and no major reliefs and hills are present in the area. The intermittent or ephemeral tributaries do have a potential influence and can contribute to mass fluxes during winter when the rainfall events mostly occur. The estimated mass flux between October and November 2008 was between 9.62 and 23.38 kg·NO_3·day^{-1}. The highest values were found in March 2009 with 85.2 kg·NO_3·day^{-1}. It can be expected that significant contributions from tributaries draining the catchment will occur, and this aspect could be subject of further research in order to develop the model.

4.2. Nitrate Sources through Isotopic Composition in Stream Waters and Wells

Biplots of the ^{15}N and ^{18}O isotopic values NO_3–N may provide some information to distinguish the different sources of nitrate. Results from dual isotopes of nitrate displayed a linearly plotted trend for stream water (slope of 0.44), indicating potential isotopic enrichment at a 1:1 ratio, related to denitrification. Figure 4 shows the isotopic composition of nitrate from different sources [16], superimposed on the values measured in the streams. The seasonal values of ^{18}O for NO_3–N were smaller than that of ^{15}N, ranging from 0.5‰ to 17.8‰ in winter and 3.5‰ to 15.6‰ in summer and autumn, with average values of 8.2‰ and 8.8‰, respectively. Mann Whitney analysis ($p < 0.05$)

revealed significant differences between ^{15}N and ^{18}O of NO_3–N of early fall and summer with respect to winter, indicating that seasonal variation of NO_3–N source affected the isotopic composition. Relative to the spatial distribution, the highest ^{18}O for NO_3–N value occurred in A9 (12.1‰), which is much higher than those of A4 and A7 (9.1‰ and 8.3‰, respectively). Low values occurred in the first site and close to the reservoir, probably due to the nitrification of sewage (site A4). Seasonal variability in nitrogen biogeochemistry was also observed in the stream, because the linear relationships between ^{18}O and ^{15}N in winter and summer were different from the denitrification trend line. The departure from the denitrification trend line in winter and summer might be the result of a change in sources.

The ranges of nitrogen and oxygen isotopic composition differ significantly between nitrate and ammonium fertilizers. The percentage of these nutrients in fertilizers in the study catchment area represent in total 1200 $kg \cdot km^{-2} \cdot year^{-1}$, with a high percentage of ammonium fertilizers added to the soil between June and August [29]. This data is crucial to the support of the reported results, as the isotopic composition of nitrate suggests that nitrification in soils was the major source of stream nitrate, consistent with the modelling results. Moreover, as indicated by Figure 4, there is a slightly sewage and manure effluents input into the stream, due to some high ^{15}N values and high ^{18}O values located downstream. Thus, while isotopic composition of nitrate from the upstream section is consistent with typical regional levels for ammonium fertilizers and soil nitrate, downstream the isotopic composition is consistent with the composition of manure septic systems and animal wastes.

Stream water ^{15}N values increased with the inverse of NO_3–N concentrations, whereas ^{15}N decreased with the natural logarithm of NO_3^-–N levels (Figure 5), probably due to a combination of mixing and fractionation associated with denitrification [8]. The nitrate may be removed by denitrification resulting in the enrichment of N and oxygen isotopic in the residual NO_3–N. Estimates of oxygen isotope fractionation during denitrification are rare [36]. However there are some studies of oxygen and nitrogen isotope enrichment factors for microbial nitrate reduction in aquatic environments [35–47]. It is reported that the ratios of $^{15}N/^{18}O$ range from -1.3 to -2.1 [48]. In our case, the microbial denitrification accords with a Rayleigh process with calculated enrichment factors of $\varepsilon = -2.9$‰ for ^{15}N and $\varepsilon = -1.5$‰ for ^{18}O. It is not uncommon to find such low values in the environment [19,49,50]. The difference in the enrichment value is commonly attributed to different substrate, temperature, denitrification rates, organic matter and biodiversity [46]. The NO_3^-–N concentration in the upstream (~17 $mg \cdot N \cdot L^{-1}$) dropped down to <0.1 $mg \cdot N \cdot L^{-1}$ (downstream). Previous studies in surface water in Roxo catchment indicated that primary productivity is relatively high in summer when high levels of nutrients are found [51] and this assimilation process may also contribute to the consumption of nitrate.

In water studies, chloride is generally used as a conservative tracer of mixing within the streams, as it is an effective indicator of sewage and dilution effects which has minimal affects from physical, chemical and biological processes [52]. Hence, the ratio of NO_3–N/Cl^- was also considered for the study of N dynamics and sources. Figure 6 shows the co-variation of NO_3–N/Cl^- ratios with Cl^- concentrations in the Chaminé stream. While most of the samples do not correspond to the ranges for sewage and manure, there are some values within this range. The lower NO_3–N/Cl^- ratios in sewage and livestock waste was partly due to the fact that they contain nitrogen that has not yet been converted to nitrate [37].

4.3. Nitrate in the Sediment Pore Waters

Generally, the decline of nitrate levels in the pore water is the results of several factors, such as dilution from additional water sources (groundwater, tributaries, etc.) or by biological processes such as denitrification and vegetation uptake [15]. The three nitrate concentration profiles in superficial sediments exhibited both horizontal and vertical spatial variability. In this study, in the first pool, pore water showed high nitrate values near the sediment-water interface (reaching 25 $mg \cdot L^{-1}$) and NO_3–N sharply decreased over depth, suggesting significant nitrate consumption in the sediment (Figure 7). Longitudinally, in the second and third pool, lower nitrate values and intensive reduction

of nitrate concentrations were found, in particular, in the vicinity of low-conductivity pore water. The concurrence of reduced oxygen concentrations and high Cl^- values in these pools suggest that increased residence times and associated depletion of dissolved oxygen generates conditions favourable for nitrate reduction. The streams in the Roxo catchment area are characterized by low flows and low water depths, mostly with high nitrate levels (around 10 $mg \cdot L^{-1}$) and DO concentrations of 7 $mg \cdot L^{-1}$, respectively. It is well known that these characteristics facilitate major ion exchange with the water-sediment interface [50,53]. However, a rapid decline in nitrate and decreasing DO occurred in the water pools. These values may indicate a strong redox pattern, and suggest the occurrence of aerobic microbal respiration followed by denitrification [15,54]. Several microcosm experiments using stream water and sediments from stream pools identified that conditions of stagnant water and low water flow velocity trigger higher denitrification rates [53]. The hypothesis the diffusion of nitrate from the shallow stream water across the sediment-water interface is the limiting step in denitrification is currently accepted, producing a low isotopic signal in the stream water [50]. Measurements of denitrification rates in Roxo catchment for downstream sediments were limited by the rate of nitrate supply (3.9 ± 2.9 $kg \cdot N \cdot ha^{-1} \cdot year^{-1}$) [26]. At these sites, the diffusion through the water sediment interface to the pore water is apparently an important process influencing the kinetics of denitrification occurring in the stream sediments.

5. Conclusions

Both the standard chemical analysis of reactive nitrogen and the stable nitrate isotope data indicated that most of the nitrogen inputs in the Roxo main stream are removed from the system and shallow waters by biogeochemical processes.

Isotopic composition of ^{15}N and ^{18}O values of surface water from the stream and wells indicated that the dominant NO_3–N sources were derived from the soil, fertilizers, manure and domestic sewage waters. There was also significant nitrification in surface waters at the head of the stream. Pore waters showed high nitrate values near the sediment-water interface (reaching 25 $mg \cdot L^{-1}$) and nitrate concentrations strongly decreased with sediment depth, suggesting significant nitrate consumption. Denitrification was also detected using the ^{15}N signature of nitrate in the surface water from the streams but not downstream near to the reservoir, where very low nitrate levels were measured.

The combination of hydrochemical and stable isotope data analysis enables the identification of sources and spatial locations of nitrogen transformation, and the removal processes in surface water systems of the catchment, as well as deepens our knowledge in on dissolved reactive nitrogen transport in aquatic systems influenced by agriculture and other human activities in this ecosystem.

Acknowledgments: This study was supported by the Faculty of Geo-Information Science and Earth Observation (ITC-UT) of the University of Twente, who financed fieldwork excursions through a PhD research grant. We gratefully acknowledge the help and data support of J. Maia of COTR, R. Nobre of Escola Agraria de Beja, A. Leal of EMAS and C. Marques of ABROXO. We thank Rafael Bermudez for logistic and technical support in the fieldwork campaigns and ITC MSc students Fransiska Gamises from Namibia, Imesh Vithanage from Sri Lanka, Imuwahen Priscilla Igbinosum from Nigeria for their contribution to the data collection and preliminary analysis work.

Author Contributions: All authors contributed to this paper with overall discussions about the research idea and designing the survey. Mariela A. Yevenes collected the data, analyzed the data and performed most of the literature review and wrote most of the paper. Karline Soetaert helped to perform the modelling of the data. Both Karline Soetaert and Chris M. Mannerts contributed to writing parts of the paper.

Conflicts of Interest: The authors declare no conflict of interest.

References

1. Gilles, J. Nitrogen study fertilizes fears of pollution. *Nature* **2005**, *433*, 791. [CrossRef] [PubMed]
2. UNEP. Reactive Nitrogen in the Environment. Available online: http://www.unep.org/pdf/dtie/Reactive_Nitrogen.pdf (accessed on 16 June 2012).

3. GANE. Global Enrichment Factor. Available online: http://www.nerc.ac.uk/research/programmes/gane/ (accessed on 6 September 2005).
4. Groffman, P.; Davidson, E.A.; Seitzinger, S. New approaches to modeling denitrification. *Biogeochemistry* **2009**, *93*, 1–5. [CrossRef]
5. NinE. Nitrogen in Europe. Available online: http://www.nine-esf.org/?q=node/205 (accessed on 4 September 2010).
6. NinE-ENA. European Nitrogen Assessment. Available online: http://www.nine-esf.org/node/204 (accessed on 4 September 2010).
7. Vitousek, P.M.; Aber, J.D.; Howarth, R.W.; Likens, G.E.; Mat-son, P.A.; Schindler, D.W.; Schlesinger, W.H.; Tilman, D.G. Alteration of the global nitrogen cycle: Sources and consequences. *Ecol. Appl.* **1997**, *7*, 737–750. [CrossRef]
8. Lohse, K.A.; Sanderman, J.; Amundson, R. Identifying sources and processes influencing nitrogen export to a small stream using dual isotopes of nitrate. *Water Resour. Res.* **2013**, *49*, 5715–5731. [CrossRef]
9. McClain, M.E.; Boyer, E.W.; Dent, C.L.; Gergel, S.E.; Grimm, N.B.; Groffman, P.M.; Hart, S.C.; Harvey, J.W.; Johnston, C.A.; Mayorga, E.; et al. Biogeochemical hot spots and hot moments at the interface of terrestrial and aquatic ecosystems. *Ecosystems* **2003**, *6*, 301–312. [CrossRef]
10. Ashkenas, L.R.; Johnson, S.L.; Gregory, S.V.; Tank, J.L.; Wollheim, W.M. A stable isotope tracer study of nitrogen uptake and transformation in an old-growth forest stream. *Ecology* **2004**, *85*, 1725–1739. [CrossRef]
11. Devol, A.H. Denitrification including anammox. In *Nitrogen in the Marine Environment*; Capone, D., Carpenter, E., Mullholland, M., Bronk, D., Eds.; Elsevier: Amsterdam, The Netherlands, 2008; pp. 263–302.
12. Wexler, S.K.; Hiscock, K.M.; Dennis, P.F. Catchment-Scale Quantification of Hyporheic Denitrification Using an Isotopic and Solute Flux Approach. *Environ. Sci. Technol.* **2011**, *45*, 3967–3973. [CrossRef] [PubMed]
13. Cabana, G.; Rasmussen, J. Comparison of aquatic food chains using nitrogen isotopes. *Proc. Natl. Acad. Sci. USA* **1996**, *93*, 10844–10847. [CrossRef] [PubMed]
14. Lake, J.L.; McKinney, R.A.; Osterman, F.A.; Pruell, R.J.; Kiddon, J.; Ryba, S.A.; Libby, A.D. Stable nitrogen isotopes as indicators of anthropogenic activities in small freshwater systems. *Can. J. Fish. Aquat. Sci.* **2001**, *58*, 870–878. [CrossRef]
15. Peyrard, D.; Delmotte, S.; Sauvage, S.; Namour, P.; Gerino, M.; Vervier, P.; Sanchez-Perez, J.M. Longitudinal transformation of nitrogen and carbon in the hyporheic zone of an N-rich stream: A combined modelling and field study. *Phys. Chem. Earth* **2011**, *36*, 599–611. [CrossRef]
16. Kendall, C.; McDonnell, J.J. *Isotope Tracers in Catchment Hydrology*; Elsevier Science: New York, NY, USA, 1998; p. 839.
17. Pintar, M.; Bolta, S.V.; Lobnik, F. Nitrogen isotope enrichment factor as an indicator of denitrification potential in top and subsoil in the Apače Valley, Slovenia. *Soil Res.* **2008**, *46*, 719–726. [CrossRef]
18. Mariotti, A.; Germon, J.C.; Hubert, P.; Kaiser, P.; Letolle, R.; Tardieux, A.; Tardieux, P. Experimental determination of nitrogen kinetic isotope fractionation: Some principles, illustration for the denitrification and nitrification processes. *Plant Soil* **1981**, *62*, 413–430. [CrossRef]
19. Søvik, A.K.; Mørkved, P.T. Use of stable nitrogen isotope fractionation to estimate denitrification in small constructed wetlands treating agricultural runoff. *Sci. Total Environ.* **2008**, *392*, 157–165. [CrossRef] [PubMed]
20. Xue, D.; Botte, J.; De Baets, B.; Accoe, F.; Nestler, A.; Taylor, P.; Van Cleemput, O.; Berglund, M.; Boeckx, P. Present limitations and future prospects of stable isotope methods for nitrate source identification in surface- and groundwater. *Water Res.* **2009**, *43*, 1159–1170. [CrossRef] [PubMed]
21. Butturini, A.; Bernal, S.; Sabater, S.; Sabater, F. The influence of riparian-hyporheic zone on the hydrological responses in an intermittent stream. *Hydrol. Earth Syst. Sci. Discuss.* **2002**, *6*, 515–526. [CrossRef]
22. Piña-Ochoa, E.; Høgslund, S.; Geslin, E.; Cedhagen, T.; Revsbech, N.P.; Nielsen, L.P.; Schweizer, M.; Jorissen, F.; Rysgaard, S.; Risgaard-Petersen, N. Widespread occurrence of nitrate storage and denitrification among Foraminifera and Gromiida. *Proc. Natl. Acad. Sci. USA* **2006**, *19*, 1148–1153. [CrossRef] [PubMed]
23. Valério, E.; Faria, N.; Paulino, S.; Pereira, P. Seasonal variation of phytoplankton and cyanobacteria composition and associated microcystins in six Portuguese freshwater reservoirs. *Ann. Limnol. Int. J. Limnol.* **2008**, *44*, 189–196. [CrossRef]

24. Otero, N.; Menció, A.; Torrentó, C.; Soler, A.; Mas-Pla, J. Multi-isotopic and hydrogeological methods applied to monitoring groundwater nitrate attenuation in a regional aquifer system (Osona, NE Spain). In *Water Pollution in Natural Porous Media at Different Scales*; Candela, L., Vadillo, I., Aagaard, P., Bedbur, E., Trevisan, M., Vanclooster, M., Viotti, P., López-Geta, J.A., Eds.; IGME: Madrid, Spain, 2007; pp. 203–209.
25. Sen, P.; Gieske, A. Use of GIS and remote sensing in identifying recharge zones in an arid catchment: A case study of Roxo river basin, Portugal. *J. Nepal Geol. Soc.* **2005**, *31*, 25–32.
26. Gamises, F. The Study of Spatial and Temporal Aspects of Denitrification Processes in Roxo Catchment, Portugal. Master's Thesis, ITC/University of Twente, Enschede, The Netherlands, 2009. p. 76.
27. Paralta, E.A.; Oliveira, M.M. Assessing and Modelling Hard Rock Aquifer Recharge Based on Complementary Methodologies—A Case Study in the Gabbros of Beja, Aquifer System (South Portugal). In Proceedings of the 2nd Workshop of the Iberian Regional Working Group on Hardrock Hydrogeology, Évora, Portugal, 18–21 May 2005; p. 15.
28. ABROXO. *Meteorological Data of Roxo Reservoir Station*; Technical Bulletin; Association of Water Users of Roxo: Beja, Portugal, 2009. (In Portuguese)
29. Yevenes, M.A.; Mannaerts, C.M. Seasonal and land use impacts on the nitrate budget and export of a mesoscale catchment in Southern Portugal. *Agric. Water Manag.* **2011**, *102*, 54–65. [CrossRef]
30. Varela, M. (Centro Operayivo e de Tecnologia de Regadio, COTR, Beja, Portugal); Nobre, R. (Escola Agraria do Beja, Portugal). Nitrogen fertilization for agricultural crops in Roxo catchment. 10 October 2008.
31. Nunes, M.E.; Paralta, E.; Cunha, M.C.; Ribeiro, L. Groundwater network optimization with missing data. *Water Resour. Res.* **2004**, *40*, W02406. [CrossRef]
32. Seeberg-Elverfeldt, J.; Schlüter, M.; Feseker, T.; Kölling, M. Rhizon sampling of porewaters near the sediment-water interface of aquatic systems. *Limnol. Oceanogr. Meth.* **2005**, *3*, 361–371. [CrossRef]
33. Casciotti, K.L.; Sigman, D.M.; Hastings, M.G.; Bohlke, J.K.; Hilkert, A. Measurement of the oxygen isotopic composition of nitrate in seawater and freshwater using the denitrifier method. *Anal. Chem.* **2002**, *74*, 4905–4912. [CrossRef] [PubMed]
34. Mariotti, A. Natural N-15 abundance measurements and atmospheric nitrogen standard calibration. *Nature* **1984**, *311*, 251–252. [CrossRef]
35. Böttcher, J.; Strebel, O.; Voerkelius, S.; Schmidt, H.L. Using isotope fractionation of nitrate-nitrogen and nitrate-oxygen for evaluation of microbial denitrification in a sandy aquifer. *J. Hydrol.* **1990**, *114*, 413–424. [CrossRef]
36. Lehmann, M.; Reichert, S.; Bernasconi, M.; Barbieri, A.; Mckenzie, J. Modelling nitrogen and oxygen isotope fractionation during denitrification in a lacustrine redox-transition zone. *Geochim. Cosmochim. Acta* **2003**, *67*, 2529–2542. [CrossRef]
37. Chen, F.; Jia, G.; Chen, J. Nitrate sources and watershed denitrification inferred from nitrate dual isotopes in the Beijiang River, South China. *Biogeochemistry* **2009**, *94*, 163–174. [CrossRef]
38. R Development Core Team. Available online: http://www.r-project.org/ (accessed on 15 July 2009).
39. Soetaert, K.; Meysman, F. Reactive transport in aquatic ecosystems: Rapid model prototyping in the open source software, R. *J. Environ. Model. Softw.* **2012**, *32*, 49–60. [CrossRef]
40. Soetaert, K.; Herman, P.M.J. *A Practical Guide to Ecological Modelling. Using R as a Simulation Platform*; Springer: Berlin, Germany, 2009.
41. Alexander, R.B.; Böhlke, J.K.; Boyer, E.W.; David, M.B.; Harvey, J.W.; Mulholland, P.J.; Seitzinger, S.P.; Tobias, C.R.; Tonitto, C.; Wollheim, W.M. Dynamic modeling of nitrogen losses in river networks unravels the coupled effects of hydrological and biogeochemical processes. *Biogeochemistry* **2009**. [CrossRef]
42. Panno, S.V.; Kelly, W.R.; Martinsek, A.T.; Hackley, K.C. Estimating background and threshold nitrate concentrations using probability graphs. *Ground Water* **2006**, *44*, 697–709. [CrossRef] [PubMed]
43. Vithanage, I. Analysis of Nutrient Dynamics in Roxo Catchment Using Remote Sensing Data and Numerical Modeling. Master's Thesis, ITC/University of Twente, Enschede, The Netherlands, 2009. p. 103.
44. Soetaert, K.; Herman, P.M.J.; Middelburg, J.J. A model of early diagenetic processes from the shelf to abyssal depths. *Geochim. Cosmochim. Acta* **1996**, *60*, 1019–l040. [CrossRef]
45. Aravena, R.; Robertson, W.D. Use of multiple isotope tracers to evaluate denitrification in ground water: Study of nitrate from a large-flux septic system plume. *Ground Water* **1998**, *36*, 975–982. [CrossRef]
46. Vander Zanden, M.J.; Vadeboncoeur, Y.; Diebel, M.W.; Jeppesen, E. Primary consumer stable nitrogen isotopes as indicators of nutrient source. *Environ. Sci. Technol.* **2005**, *39*, 7509–7515. [CrossRef] [PubMed]

47. Brandes, J.A.; Devol, A.H. Isotopic fractionation of nitrogen and oxygen in coastal marine sediments. *Geochim. Cosmochim. Acta* **1997**, *61*, 1793–1801. [CrossRef]
48. Mengis, M.; Schiff, S.L.; Harris, M.; English, M.C.; Aravena, R.; Elgood, R.J.; MacLean, A. Multiple geochemical and isotopic approaches for assessing groundwater NO_3-elimination in a riparian zone. *Ground Water* **1999**, *37*, 448–457. [CrossRef]
49. Lund, L.J.; Horne, A.J.; Williams, A.E. Estimating denitrification in a large constructed wetland using stable nitrogen isotopes. *Ecol. Eng.* **2000**, *14*, 67–76. [CrossRef]
50. Sebilo, M.; Billen, G.; Grably, M.; Mariotti, A. Isotopic composition of nitrate-nitrogen as a marker of riparian and benthic denitrification at the scale of the whole Seine River system. *Biogeochemistry* **2003**, *63*, 35–51. [CrossRef]
51. Mateus, M.; Almeida, C.; Brito, D.; Neves, R. From Eutrophic to Mesotrophic: Modelling Watershed Management Scenarios to Change the Trophic Status of a Reservoir. *Int. J. Environ. Res. Public Health* **2014**, *11*, 3015–3031. [CrossRef] [PubMed]
52. Zeng, H.; Wu, J. Tracing the nitrate sources of the Yili River in the Taihu Lake Watershed: A dual isotope approach. *Water* **2015**, *7*, 188–201. [CrossRef]
53. Eriksson, P.D. Interaction effects of flow velocity and oxygen metabolism on nitrification and denitrification in biofilms on submersed macrophytes. *Biogeochemistry* **2001**, *55*, 29–44. [CrossRef]
54. Hedin, L.O.; von Fischer, J.C.; Ostrom, N.E.; Kennedy, B.P.; Brown, M.G.; Robertson, G.P. Thermodynamic constraints on nitrogen transformations and other biogeochemical processes at soil-stream inter-faces. *Ecology* **1998**, *79*, 684–703.